Veröffentlichung

Autoren

Mößner, Michael;Radespiel, Rolf

Titel

Implementation of Flow through Porous Media into a Compressible Flow Solver

Publisher o. Konferenz

New Results in Numerical and Experimental Fluid Mechanics IX, ISBN 978-3-319-03157-6, Volume 124 , Springer International Publishing, page 465-473

Jahr

2014

Internet-Link (Doi-Nr.)

Implementation of Flow through Porous Media into a Compressible Flow Solver

Michael Mößner and Rolf Radespiel

Technische Universität Braunschweig
Hermann-Blenk-Straße 37, 38108 Braunschweig
m.moessner@tu-bs.de, r.radespiel@tu-bs.de

Abstract. A method for simulating turbulent compressible flow through porous material is presented. The demonstration is based on spatial and time averaging of the Navier-Stokes equations. The averaging procedure leads to additional terms which have to be modelled. The integration of the resulting theory into the flow solver DLR TAU is explained. The extended code is verified by analytical solutions which are used as reference.

1 Introduction

Airplane noise during lift off and approach is is a huge problem for the environment. This is why noise reduction gains high attention by researchers besides the other well known area of increasing efficiency. One way to make airplanes quieter is shown experimentally by Herr in [1]: A significant reduction of noise is achieved by making the trailing edges of the wing porous. As a side effect, the added porous regions can alter the flow around the wing (see figure 1). This paper shows a way to integrate porous media simulation capabilities into compressible flow solvers used for aeronautical applications to enable them simulating the modified flow.

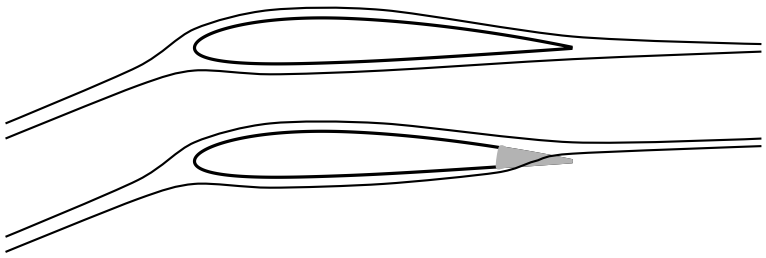

Fig. 1. Upper: airfoil with solid trailing edge, lower: airfoil with porous trailing edge which is permeable.

2 Derivation of the Porous Transport Equations

At present, in most technical relevant simulations flow inside the single pores of a porous material cannot be resolved. This problem can be overcome by spatial averaging. Instead of simulating the flow through the pores it models the porous effect homogeneously. A similar procedure is used for turbulence. The turbulence is not resolved rather its effect is taken into account by averaging in time and modelling the Reynolds stresses. The basic strategy for spatial averaging in incompressible flow can be found in [2]. The procedure for obtaining nonporous turbulence equations is described in [3] extensively. The two principles are used in the present paper to obtain the compressible RANS equations which are valid inside and outside porous media. To keep the equations simple density weighted averaging is used. The final equations result in

$$\frac{\partial \overline{\rho}}{\partial t} + \frac{\partial \overline{\rho}\widetilde{v_k}}{\partial x_k} = 0 \quad \text{(1a)}$$

$$\frac{\partial \overline{\rho}\widetilde{v_i}}{\partial t} + \frac{\partial \overline{\rho}\widetilde{v_i}\widetilde{v_k}}{\partial x_k} + \frac{\partial \overline{\rho}\widetilde{v_i''v_k''}}{\partial x_k} + \frac{\partial \overline{p}}{\partial x_i} - \frac{\partial \overline{\tau_{ik}}}{\partial x_k} + \phi\frac{\mu}{\kappa}\widetilde{v_i} + \overline{\rho}\frac{c_F}{\sqrt{\kappa}}\widetilde{\sqrt{v_k v_k}v_i} = 0 \quad \text{(1b)}$$

$$\frac{\partial \overline{\rho}\widetilde{e}}{\partial t} + \frac{\partial \frac{1}{2}\overline{\rho}\widetilde{v_j}\widetilde{v_j}}{\partial t} + \frac{\partial \frac{1}{2}\overline{\rho}\widetilde{v_j''v_j''}}{\partial t} + \frac{\partial \overline{\rho}\widetilde{h}\widetilde{v_k}}{\partial x_k} + \frac{\partial \overline{\rho}\widetilde{h''v_k''}}{\partial x_k} + \frac{\partial \frac{1}{2}\overline{\rho}\widetilde{v_j}\widetilde{v_j}\widetilde{v_k}}{\partial x_k} \quad \text{(1c)}$$
$$+\frac{\partial \frac{1}{2}\overline{\rho}\widetilde{v_k}\widetilde{v_j''v_j''}}{\partial x_k} + \frac{\partial \overline{\rho}\widetilde{v_j}\widetilde{v_j''v_k''}}{\partial x_k} + \frac{\partial \frac{1}{2}\overline{\rho}\widetilde{v_j''v_j''v_k''}}{\partial x_k} - \frac{\partial \widetilde{v_j}\overline{\tau_{jk}}}{\partial x_k} - \frac{\partial \overline{v_j''\tau_{jk}}}{\partial x_k} - \frac{\partial \overline{k_{d,k}}}{\partial x_k} = 0$$

by using the Einstein notation. All variables are spatially averaged which is not labelled explicitly. The Favré average in time is marked with a tilde, the fluctuation with two primes: $\varphi = \widetilde{\varphi} + \varphi''$. In the equations, v is the velocity, p is the pressure, τ is the tensor of viscous stresses, e is the internal energy, h is the enthalpy, k_d is the thermal diffusion and μ is the dynamic viscosity. The porous variables are the porosity ϕ, permeability κ and the Forchheimer coefficient c_F.

The following simplifications which were used: The correlations between spatial fluctuations are negligible ([2]) and the additional integrals which appear after spatial averaging can be modelled by the Darcy- and Forchheimer term. A further simplification of the energy equation is setting the thermal diffusion at the pore surfaces to zero.

The correlations in the energy equation (1c) are not investigated any further here. Basically, they can be modelled with a turbulent Prandtl number Pr_t and the eddy viscosity μ_t. The main difficulty to be solved is finding an approximation for the Forchheimer term $\overline{\rho}\frac{c_F}{\sqrt{\kappa}}\widetilde{\sqrt{v_k v_k}v_i}$ and the derivation of the Reynolds stresses $\widetilde{v_i''v_k''}$.

Getachew, Minkovycz and Lage ([4]) use a Taylor expansion to approximate the Forchheimer term. Inhere, a Taylor expansion is used in a similar way but resulting from a slightly different approach ($v_i = x\widetilde{v_i}$ where x at the reference point is 0 and the deviation from the reference point is 1) the final approximation

contains more terms:

$$\overline{\rho}\frac{c_F}{\sqrt{\kappa}}\widetilde{\sqrt{v_k v_k}v_i} = \overline{\rho}\frac{c_F}{\sqrt{\kappa}}\left[\sqrt{\widetilde{v_l}\widetilde{v_l}}\cdot\widetilde{v_i} + \frac{1}{2}\frac{\widetilde{v_i}}{\sqrt{\widetilde{v_l}\widetilde{v_l}}}\widetilde{v_j''v_j''} + \frac{\widetilde{v_j}}{\sqrt{\widetilde{v_l}\widetilde{v_l}}}\widetilde{v_i''v_j''} - \frac{1}{2}\frac{\widetilde{v_i}\widetilde{v_j}\widetilde{v_k}}{\sqrt{(\widetilde{v_l}\widetilde{v_l})^3}}\widetilde{v_j''v_k''}\right] . \tag{2}$$

The remaining unknows are the Reynolds stresses which have to be modelled. The modelling is done by introducing Reynolds stress transport equations. Following the principle of Wilcox in [3] and taking into account the effects of porosity the resulting Reynolds stress equations are

$$\frac{\partial\overline{\rho}\widetilde{v_i''v_j''}}{\partial t} + \frac{\partial\overline{\rho}\widetilde{v_k}\widetilde{v_i''v_j''}}{\partial x_k} = P_{ij} + \Phi_{ij} + D_{ij} + \varepsilon_{ij} - \overline{v_j''}\frac{\partial\overline{p}}{\partial x_i} - \overline{v_i''}\frac{\partial\overline{p}}{\partial x_j} - \mathcal{D}_{\mathrm{RS}} - \mathcal{F}_{\mathrm{RS}} \tag{3}$$

where P_{ij} is the production term, Φ_{ij} is the redistribution term, ε_{ij} is the dissipation and D_{ij} stands for diffusion. These equations also show the extension due to the Darcy term

$$\mathcal{D}_{\mathrm{RS}} = \phi\frac{\mu}{\kappa}\left[\overline{v_i''}\widetilde{v_j} + \overline{v_j''}\widetilde{v_i} + 2\overline{v_i''v_j''}\right] \tag{4}$$

and the extension caused by the Forchheimer term

$$\begin{aligned}\mathcal{F}_{\mathrm{RS}} = \frac{c_F}{\sqrt{\kappa}}\overline{\rho}\Bigg[&2\widetilde{v_i''v_j''}\sqrt{\widetilde{v_l}\widetilde{v_l}} + \frac{\widetilde{v_j}\widetilde{v_k}}{\sqrt{\widetilde{v_l}\widetilde{v_l}}}\widetilde{v_i''v_k''} + \frac{\widetilde{v_i}\widetilde{v_k}}{\sqrt{\widetilde{v_l}\widetilde{v_l}}}\widetilde{v_j''v_k''} + 2\frac{\widetilde{v_k}}{\sqrt{\widetilde{v_l}\widetilde{v_l}}}\widetilde{v_i''v_j''v_k''} \\ &+ \frac{1}{2}\frac{\widetilde{v_j}}{\sqrt{\widetilde{v_l}\widetilde{v_l}}}\widetilde{v_i''v_k''v_k''} + \frac{1}{2}\frac{\widetilde{v_i}}{\sqrt{\widetilde{v_l}\widetilde{v_l}}}\widetilde{v_j''v_k''v_k''} \\ &- \frac{1}{2}\frac{\widetilde{v_j}\widetilde{v_m}\widetilde{v_k}}{\sqrt{(\widetilde{v_l}\widetilde{v_l})^3}}\widetilde{v_i''v_m''v_k''} - \frac{1}{2}\frac{\widetilde{v_i}\widetilde{v_m}\widetilde{v_k}}{\sqrt{(\widetilde{v_l}\widetilde{v_l})^3}}\widetilde{v_j''v_m''v_k''}\Bigg] .\end{aligned} \tag{5}$$

The influence of the Forchheimer term shown here is a Taylor expansion with 2nd order accuracy.

3 Modelling of the Interface Region

The derivation of the Navier-Stokes-equations in porous materials underlies the assumption of constant porosity ϕ. This condition does not hold at the interface area between porous and nonporous flow. As a consequence, the interface region has to be modelled. For flow directions normal to the interface plane an isentropic

flow change is used:

$$\text{Mass conservation:} \quad \rho_f \cdot v_{n,f} = \phi \cdot \rho_p \cdot v_{n,p} \tag{6a}$$

$$\text{Energy conservation:} \quad \frac{\gamma}{\gamma-1}\frac{p_f}{\rho_f} + \frac{v_f^2}{2} = \frac{\gamma}{\gamma-1}\frac{p_p}{\rho_p} + \frac{v_p^2}{2} \tag{6b}$$

$$\text{Isentropic condition:} \quad \frac{p_f}{\rho_f^\gamma} = \frac{p_p}{\rho_p^\gamma} \tag{6c}$$

The index f labels the nonporous flow and p marks porous flow. v_n is the flow velocity perpendicular to the interface and γ is the isentropic exponent. The equations are solved by the Newton method.

According to literature ([2]) the velocities v_t tangential to the interface are related as follows:

$$v_{t,f} = v_{t,p} \cdot \phi \tag{7}$$

This relation should be proven for compressible flow but is adopted here in order to compare the solution with analytical results available.

The widely acknowledged strategy to overcome the error of the interface models is the use of a stress jump at the interface ([2], [5]):

$$\mu \cdot \frac{\partial v_{t,f}}{\partial n} - \mu \cdot \frac{\partial v_{t,p}}{\partial n} = \beta\phi\frac{\mu}{\sqrt{\kappa}} v_{t,f} \tag{8}$$

with $\frac{\partial}{\partial n}$ being the derivative in interface normal direction and β as the jump coefficient of order 1. The jump condition can be seen as an additional source term at the interface which corrects the Darcy term.

4 Integration into the DLR Flow Solver TAU

The DLR TAU Code ([6]) is an unstructured flow solver based on the finite volume method. There are three implementation issues to provide the code with porous computation capabilities. First of all, volume source terms (Darcy- and Forchheimer) are added to the residuals of porous volume cells. This has the effect of additional flow drag inside the porous region.

Computing the fluxes at the nonporous–porous interface is implemented as central scheme. To determine the flux into the porous cell the states of the contacting nonporous cell (v_f, p_f, ...) are first transformed into dummy porous cell states ($v_{f,i}$, p_{v_i},...) which are compatible with the porous states. The transformation is accomplished by equations (6) and (7) (see also figure 2). The central scheme for computing the mass flux $\dot{m}$ into the porous cell is then

$$\dot{m}_{\text{porous}} = \frac{1}{2}\left(\rho_p \cdot v_{n,p} + \rho_{f,i} \cdot v_{n,f,i}\right) \cdot A \cdot \phi \ . \tag{9}$$

The same scheme is applied to the momentum and energy equations over the interface. The viscous forces also need a transformation of velocity gradients.

They are scaled by the relation

$$\frac{\partial v_{f,i}}{\partial x_j} = \frac{v_f}{v_{f,i}} \cdot \frac{\partial v_f}{\partial x_j} \ . \tag{10}$$

The flux into the nonporous interface cell is determined the same way as described for the flux into the porous cells but with the porous flow conditions transformed to nonporous conditions (figure 2 to the bottom right).

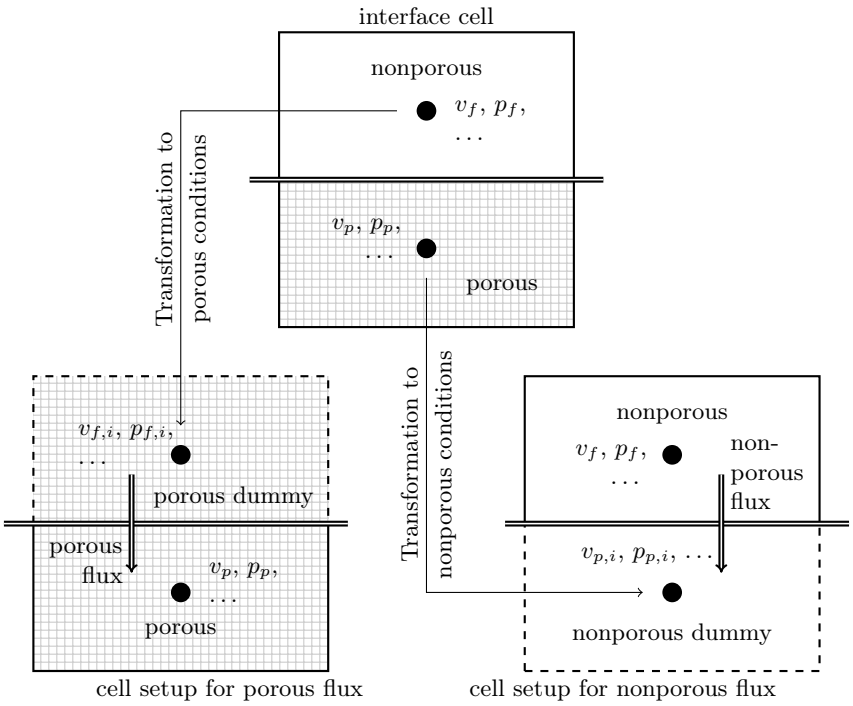

Fig. 2. Flux computation at nonporous–porous interface. Transformation to porous/nonporous conditions is based on equations (6) and (7).

The third step of integrating porous material into TAU is correcting the residuals of the interface cells to fulfill the jump condition (8). This is accomplished by adding an additional force as source term to both interface cells. The additional force leads to a kink in the velocity profile which is equal to a stress jump (see figure 3).

5 Verification Computations

As first verification experiment which can be compared easily with well known solutions serves a channel flow where the first part is nonporous and the second

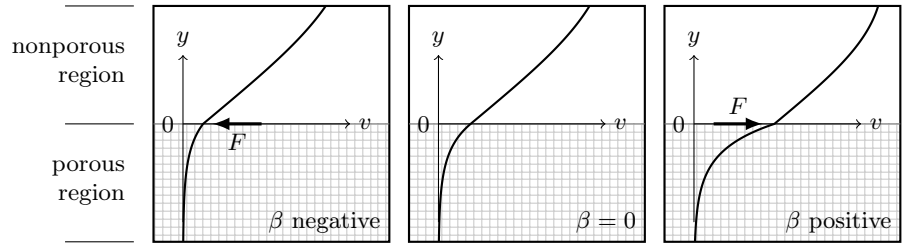

Fig. 3. Correction of boundary layer shape by additional source term to fulfil the jump condition.

part is filled completely with porous material. It is clear that as long as the flow is incompressible the velocity between the pores has to increase by the factor of $\frac{1}{\phi}$ as the effective flow area decreases by the factor of ϕ. If the channel walls are defined using slip wall boundary conditions pressure losses will only occur inside the porous region. The theoretical pressure decrease can be compared with the theory of Darcy. The results using the modified TAU-Code are demonstrated in figure 4. As the porosity ϕ is 0.5, the velocity doubles from 2.6 $\frac{\mathrm{m}}{\mathrm{s}}$ to 5.6 $\frac{\mathrm{m}}{\mathrm{s}}$ at the nonporous–porous interface. There is also a small pressure jump at the interface which is hard to see due to the low kinetic energy in the flow. However, the effect of the pressure drop inside the porous region is visible very well. The theory of Darcy yields

$$\Delta p = \phi \cdot \frac{\mu}{\kappa} \cdot v_p \cdot l_{\mathrm{channel}} = 0.5 \cdot \frac{1.74 \cdot 10^{-5}\ \frac{\mathrm{kg\,s}}{\mathrm{m}}}{1 \cdot 10^{-8}\ \frac{1}{\mathrm{m}^2}} \cdot 5.7\,\frac{\mathrm{m}}{\mathrm{s}} \cdot 1\,\mathrm{m} = 4959\,\frac{\mathrm{N}}{\mathrm{m}^2}\ . \quad (11)$$

The pressure drop on the CFD results is 4947 $\frac{\mathrm{N}}{\mathrm{m}^2}$ which is almost equal. The small difference occurs as the CFD results are based on compressible equations.

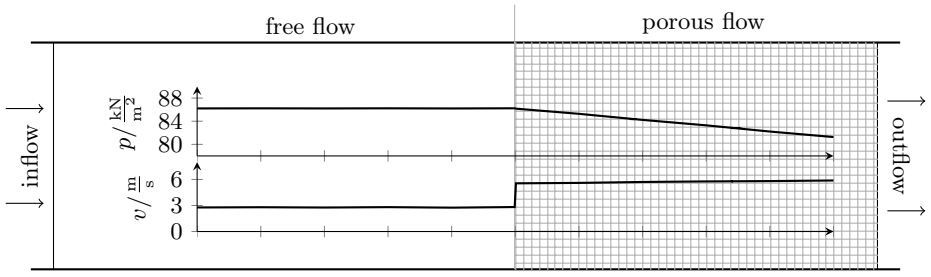

Fig. 4. Channel flow with the right part being filled with porous material (porosity $\phi = 0.5$). The diagrams show the pressure p and velocity v along the channel.

An evaluation of a boundary layer flow can serve as a second verification case. Breugem [2] showed an analytical way for computing a laminar boundary layer

over a porous region. His theory is based on the Blasius boundary layer with a porous wall correction. The ordinary differential equations which describe the boundary layer are

$$f_0''' + f_0 f_0'' = 0 \tag{12a}$$
$$f1''' + f_1'' f_0 + f_0' f_1' = 0 \tag{12b}$$

with the boundary conditions

$$\begin{aligned} \eta = 0: \quad & f_0' = 0 \quad & f_1' = f_0'' \\ & f_0 = 0 \quad & f_1 = 0 \\ \eta \to \infty: \quad & f_0' \to 1 \quad & f_1' \to 0 \end{aligned}$$

and are solved by a shooting method. The dimensionless variables f_0, f_1 and η define the wall distance y and flow velocity v according to

$$y = \eta \cdot \delta \qquad \text{with } \delta = \sqrt{2\frac{x \cdot \mu V_\infty}{\rho}}$$
$$v_{\text{nonporous}} = V_\infty \cdot (f_0' + \kappa f_1')$$
$$v_{\text{porous}} = \frac{1}{\phi} V_\infty f_1'(0) \cdot e^{\left(\frac{\sqrt{\phi}\eta}{a \cdot b}\right)} \qquad \text{with } a = \frac{1}{\sqrt{\phi}} - \beta \text{ and } b = \frac{\sqrt{K}}{a\delta}$$

A comparison of the analytical results with the TAU solutions is shown in figure 5. The differences between the two curves are very small demonstrating the correct TAU implementation.

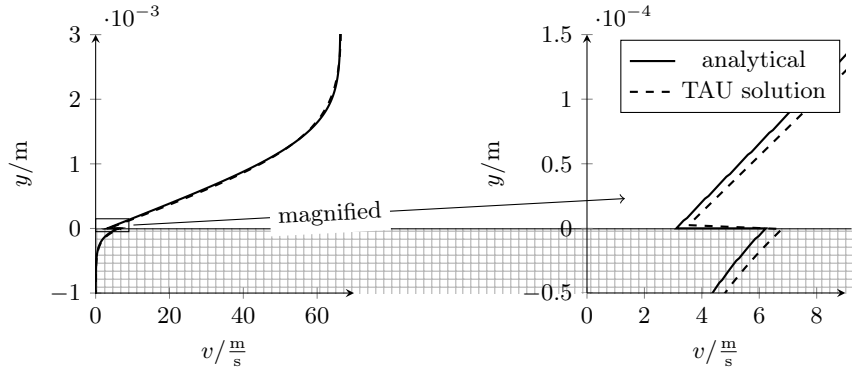

Fig. 5. Comparison of porous boundary layers at a jump coefficient $\beta = 0$.

6 Conclusion

A theory to compute compressible flow through porous material has been presented. That includes the Reynolds stress equation in porous material which are needed for turbulent flows. The basic principles for the derivation of the equations are spatial and time averaging. This procedure avoids the need for resolving the porous structure and the turbulent time scales. Instead unknown terms are emerging which are modelled by the Darcy and Forchheimer term. These terms can also be found in the Reynolds stress equations which are needed for turbulence modelling.

Besides the modelling of terms inside the porous material the interface region between nonporous and porous flow has to be modelled in a suited way. This is necessary as the porosity is not constant at the interface region. The modelling strategy is the assumption of isentropic flow change over the interface area. The error which occurs through the assumptions is compensated by a stress jump condition which conforms with literature.

The theoretical derivations are followed by a description about the implementation of the equations into a flow solver. Virtual states have to be computed at the interface to determine the fluxes. The implementation is verified by channel and boundary layer flows. Therefore, reference cases can be found in the literature which show the implementation to be correct.

Further verifications will need DNS computations to prove the models used are valid. Especially, the interface conditions tangential to the wall have to be checked. Turbulent cases will also be verified in future.

The resulting extension of the TAU code will provide the ability to predict the aerodynamic behaviour of shapes like airfoils and wings with porous regions.

References

1. Herr, M.: Design criteria for low-noise trailing-edges, DLR, German Aerospace Center, 38108 Braunschweig (2007)
2. Breugem, W.P.: The influence of wall permeability on laminar and turbulent flows. PhD thesis, Technische Universiteit Delft (1 2005)
3. Wilcox, D.C.: Turbulence Modeling for CFD. 3 edn. DCW Industries (2006)
4. Getachew, D., Minkowycz, W.J., Lage, J.L.: A modified form of the κ-ε model for turbulent flows of an incompressible fluid in porous media. International Journal of Heat and Mass Transfer **43** (2000) 2909–2915
5. de Lemos, M.J.S., Silva, R.A.: Turbulent flow over a layer of a highly permeable medium simulated with a diffusion-jump model for the interface. International Journal of Heat and Mass Transfer **49** (2006) 546–556
6. Schwamborn, D., Gerhold, T., Heinrich, R.: The dlr tau-code: Recent applications in research and industry. In Wesseling, P., Oñate, E., Périaux, J., eds.: ECCOMAS CFD 06, TU Delft, The Netherlands (9 2006)